Numerical Investigation of the Attenuation of Shock Waves by Simulating a Second, Transient Medium to Protect Vehicles Against Blasts

Burghard Hillig, Arash Ramezani, Hendrik Rothe
Chair of Measurement and Information Technology
University of the Federal Armed Forces
Hamburg, Germany
Email: burghard.hillig@hsu-hh.de, ramezani@hsu-hh.de, rothe@hsu-hh.de

***Abstract*—This paper describes the numerical investigations of a directed blast of 12.5 kg Pentaerithrytoltetranitrate and a 2.6 kg Trinitrotoluene heavy mortar grenade. The propagation of the resulting shock wave in the direction of a vehicle model is investigated. Various changes of the properties of the surrounding air have been made to produce a second, transient medium. The results are intended to answer the question as to whether and to what extent the rapid heating of ambient air offers the possibility to attenuate the amplitude of an approaching shock wave. A developed test set-up was used to simulate and record the pressure profiles by simulated pressure gauges. To get an optimal configuration, a parameter study of the properties of the second medium has been performed. As a result, as well in the case of 12.5 kg explosive ordnance as with the heavy mortar grenade, a reduction of the peak overpressure compared to the undisturbed propagation of the shock wave could be determined by about 35 % when heated rapidly to 3000 K.**

Keywords–shock wave; attenuation; blast; vehicle protection; ANSYS AUTODYN.

I. INTRODUCTION

In this paper, the theoretical feasibility of an attenuation method for shock waves is further investigated by using numerical simulation software. The first work in this area was done by fundamental considerations, creation and simulation of a basic problem set-up [1]. Especially, the idea of forming an attenuation space out of air to protect vehicles was evaluated. This idea is based on a patent [2]. An effect of this patent was a discussion and the preceding simulation about the possibility to create a weakening mechanism against blasts like some sort of attenuation shield. Such a shield would be an effective safeguard against the threats that the armed forces are facing in today's operations.

Today's military operations differ in earlier times particularly in the fact that the stabilization of countries and peacekeeping have taken a much larger share. These operations vary in intensity, duration, environment, risk and involvement with the civilian population [3] [4]. The aim of these missions is to stabilize a failed or newly formed state. Another possibility is the reconstruction of a state after war. For that, it is necessary to establish a peaceful and stable environment for the citizen as well as for all executive elements. In order to fulfill these missions, not only military armed forces provide security but also civilian security forces, including police, personal security and private security personnel.

Besides these stabilizing operations abroad, the number of deployments taking place within stable countries and normal peaceful conditions has increased in recent years. This development was triggered by an increase of religiously and politically motivated terrorist attacks and disruptive actions. The aim of these actions is to intimidate the population, civil aid organizations, regular army and security forces through terror. Terrorists of this kind are using explosives by means of improvised explosive devices (IEDs) to achieve their goals. This tactic has been used in many different countries and from numerous terrorist and criminal organizations [5]. Such a terrorist threat or incident can occur at any time of day with little or no warning and may result in casualties and heavy damage. Furthermore, terrorists can also use high-angle weapons with explosive ammunition, such as mortars, in order to conceal and flexibly carry out attacks on security forces.

This development results in an increased need for protection against explosive weapons for all armed and security forces. For military forces, the protection of existing armor and protective systems is already at a high level. Nevertheless, this protection is primarily designed for direct fire, splitter and shrapnel. Shrapnel are metal fragments which are flung away by the explosion of an explosive charge. But these damage effects represent only a part of the entire damage and can be handled by physical barriers such as armors.

Another damage effect is caused by the shock wave of the explosion. A shock wave is a very fast moving, strong pressure wave which is created in air by a rapid release of energy [6]. Its state variables pressure, temperature and density change almost instantaneously. The shock wave passes through surrounding air with a high velocity and with practically no resistance. If the shock wave has contact with other media during its propagation, it can be traversed by the shock wave. Physical barriers, which protect against splitter, offer little or no protection against shock waves. That is because the abrupt pressure change of the shock wave can overcome the barrier.

In order to protect people, vehicles and structures from the destructive forces of shock waves, the peak overpressure and

the rapid pressure increase of the shock wave must be reduced. Such a reduced pressure could make a major contribution to the protection of structures, vehicles and personnel of the armed forces and security forces.

In this paper, the theoretical feasibility of an attenuation method for shock waves is tested by using the numerical simulation software ANSYS AUTODYN (Canonsburg, USA). Especially the idea of forming an attenuation space to protect vehicles is evaluated.

After this introduction, Section II of this paper presents an overview about general properties of shock waves and methods of shock wave attenuation, followed by Section III about numerical simulation, spatial discretization and material models. Section IV describes the basic and advanced problem set-up for the simulation. The results of this problem set-up with respect to any attenuation will be discussed in Section V. This paper ends with a conclusion section.

A. Background and Methods

This section describes the general, theoretical properties of shock waves and is intended to provide an overview of existing ways to attenuate shock waves. In addition, the idea of an attenuation method is explained, which is examined in this paper for feasibility.

1) General Shock Wave Properties: When an explosion is initiated in a gas, a very rapid exothermic chemical reaction occurs. As the reaction proceeds, a part of the energy of the explosive material is released very fast. As source of energy of this reaction, a multitude of materials can be used in a wide range of aggregate states. Some well-known examples of solid explosive materials are Trinitrotoluene (TNT) and Pentaerithrytoltetranitrate (PETN). But also the stored energy within a compressed, cold or hot gas can be such an energy source.

The explosive products initially expand at very high velocities and reach equilibrium with the surrounding air [7]. The properties of air as a compressible gas result in a shock wave that propagates in time. Such a wave differs from a sound wave where the displacements of the gas molecules are very small. Instead, the displacements of a shock wave have a finite value. The result is a non-linear wave in which the sound speed is related to the amplitude. The disturbances caused by the energy release travel faster than the surrounding fluid can react due to its specific sound speed. As a consequence, there is a instantaneous change of the properties of the fluid. Some examples of these properties are density, pressure and temperature. In that way, a wave front is created which consists of strongly compressed air and moves radially away from the source at supersonic velocity.

If the shock wave is caused by a detonation of an explosive charge, it is called a blast wave. This name arises from the strong wind that accompanies the wave and is felt by a stationary observer as the wave passes. In addition, the term shock wave is generally used to describe a steep pressure gradient in which the wave pattern is not characterized in detail [8].

The behavior of a shock wave can be described by a time-dependent pressure profile. After a certain time t_a the shock wave reaches a point in space, the pressure will increase rapidly from ambient air pressure P_0. The increase in pressure reaches a maximum peak pressure value P_pop and decreases after that. Figure 1 shows the described time-dependent pressure profile of an ideal shock wave as red curve. Due to the proceeding expansion of the shock wave, the wave will geometrically occupy an increasingly larger space. Because the crossed air is heated by the shock wave, a part of its energy will be dissipated as heat. That is why, the positive pressure drops exponentially. This is referred as positive phase which ends after the duration t_d. As the shock wave continues to expand, the pressure at a point in space is reduced to values below P_0. These values asymptotically approaches the atmospheric pressure P_0 over time and enter into a state of equilibrium with the surrounding air. This is referred as negative phase.

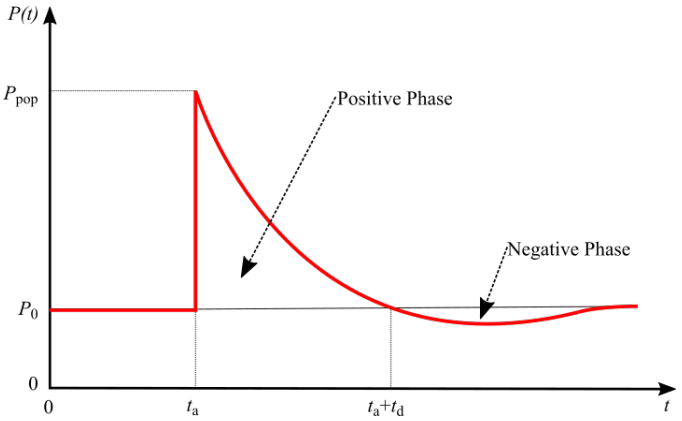

Figure 1. Characteristic time-dependent pressure profile of an ideal shock wave as a red curve. After the explosion, the wave propagates in space and reaches a point after the "time of arrival" t_a.

The easiest way to mathematically describe the pressure profile of a shock wave in air is the Friedlander equation [9]:

$$P(t) = P_0 + P_\mathrm{pop} \cdot \left(1 - \frac{t}{t_\mathrm{d}}\right) \cdot \mathrm{e}^{-\frac{t}{t_\mathrm{d}}} \qquad (1)$$

In this equation, P_0 is the atmospheric pressure,t the time and t_d the duration of the positive phase. In this case, the positive peak overpressure P_pop is the value of pressure at the pressure peak subtracted by the atmospheric pressure. The Friedlander equation is valid only from the time of arrival t_a.

2) An Overview of Shock Wave Attenuation: The idea of shock wave attenuation to protect stationary or moving objects is not new. For structures such as bunkers or tunnel systems, shock waves can be weakened by being forced into structural channels. These channels cause multiple abrupt changes of the propagation direction of the shock wave. Also, reflections of

the wave on rough walls contribute to the attenuation by the disturbance of the unimpeded propagation [10]. If the object is endangered by shock waves on its exterior side, other methods must be used to protect the object.

Therefore, there is the possibility to attenuate the shock wave by bringing in a material between shock wave and object. This material may have the property of absorbing energy from the shock wave. An example of a realization of such a absorber is a porous material, which covers the entire surface of an object to be protected [11] [12]. A very similar protection concept can be achieved by a number of cells containing the attenuating material and placed on the surface [13]. Also, heavy but transportable attenuation shields are a feasible way to attenuate the propagation of the shock wave and thus protect persons [14].

A disadvantage of all of this methods is that the shock wave attenuating material has to be permanently applied on a structure, surface or person or it must at least be close to the object.

3) Suggested Method of Shock Wave Attenuation: The creation of a second, transient medium offers a dynamical method for shock wave attenuation. This second medium shall be created in a region between the site of explosion and the asset to be protected. It can be made by placing small solid particles or fine liquid droplets in a gas phase [15]. The density of air in this volume is lower but the overall density is higher. Compared to air the solid particles have a higher density and the more particles are in a volume the higher its density. A medium created in this way has a higher density than the surrounding air. It can be observed that a crossing shock wave is attenuated through this dust-gas-suspension [16].

Such an attenuation can also be achieved if the second medium is not a suspension. This can be accomplished through rapid heating of a volume of air between the shock wave and the object [2]. By that, the heated air creates a medium, which differs in density, temperature or composition from the surrounding air. Such a medium should reduce the energy density of the crossing shock wave by reflecting a part of the shock wave on the interface between the media. Another part of the shock wave could be scattered away from its original propagation direction. In addition, the wave front can be influenced to diverge within the second medium and gets partly absorbed. In this way, the entire shock wave should be weakened.

To accomplish the attenuation of an approaching blast wave in reality, it is necessary to have a system which offers the capability to detect an explosive event, determine its direction and propagation velocity. Subsequently, the system has to create a second, transient medium to protect an asset. This second medium has to be placed between shock wave and the object. Furthermore, the medium should be formed by rapidly heating a zone of the surrounding, ambient air.

From a technical point of view, such a system should include a sensor for detecting the source of the shock wave, a computer system for processing the detected signal, and a triggering countermeasure communicating with the detection system. In Figure 2, a sketch of this system is shown based on the previously cited patent. The asset to be protected can be a military or a civil safety vehicle. The described countermeasure has the task to create a second medium by heating the surround air, which depends on the position relative to the asset to be protected, the spatial expansion and the composition. The heating of this intermediate region can be realized through an electromagnetic arc. Through this electrical arc, an electric current can flow through air by using a conductive path which is made by the dielectric collapse of the ionized air. Other possible ways to archive this heating are by focused microwaves or laser beams.

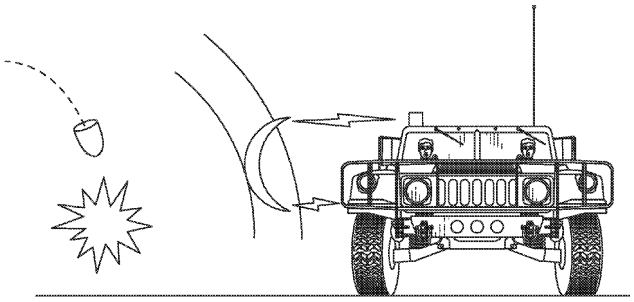

Figure 2. Sketch of a vehicle and an explosive event. The vehicle protects itself by activating a countermeasure which creates an second, transient medium by heating the ambient air between the explosion and the vehicle. Adapted from [2].

The surround air can also be heated without an electric arc by using multiple conductive strips or threads. Starting from an energy source, a very strong electric current is sent into the conductive material, so that it evaporates and strongly heats the air.

In principle, the presented method for attenuating shock waves can be applied to all types of vehicles, fixed structures, airplanes and also ships. However, for the subsequent investigations, the technical realization of the attenuation space is not a priority. Instead, numerical simulations with the software ANSYS AUTODYN are used to investigate the theoretical feasibility and verifiability of a blast wave attenuation by using the described effect of a rapidly, heated region of air.

II. Numerical Simulation

This section explains the basic principles of numerical simulation and describes the material models used in this work.

A. Spatial Discretization

When it comes to solving problems related to the release of huge amounts of energy in very short time then different

solutions are possible. A good possibility to describe such processes offer analytical solutions. Unfortunately, their applicability is limited to problems with simple geometries and few boundary and initial conditions. Numerical simulations, on the other hand, offer a solution to common problems and deal with difficulties related to geometry [17].

The basic physical model of a numerical simulation can be attributed to physical conservation laws, the equation of state and the constitutive model. Partial differential equations for energy, momentum and mass constitute the physical conservation laws. Furthermore, the equation of state connects the internal energy respectively temperature and density of a material with its pressure. As a result, changes in the density and irreversible thermodynamic processes such as shock-like heating can be considered. In addition, the constitutive model contains the effects of the material to be simulated and describes the effect of change in shape and material strength properties.

Together, these equations build a set of coupled, time- and space-dependent, highly non-linear partial differential equations. These governing partial differential equations must be solved in both time and space domain. The solution can be achieved via computer simulations with an explicit method, in which the solution is expressed at a given time as a function of the system variables and parameters, without stiffness and mass matrix requirements. The computation time for every time step is low, but may require numerous time steps for a complete solution. The solution for the space domain can be achieved by using different spatial discretization methods, like Lagrange [18], Euler [19], Arbitrary Lagrange-Euler [20] or a mesh free method [21]. Each of this methods has its unique advantages but also limitations. So, normally there is no single technique, which handles every part of the problem correctly [22].

In the presented work, two of these methods are used for spatial discretization: the Lagrange and Euler method. The Lagrange method is used to model objects. In return, the multi-material Euler solver is used to model air and the explosive.

1) Lagrange: The Lagrange method divides an object into a spatial grid, which is bound rigidly to the object and moves with it. The material component within an element does not change. If forces are acting on a node of an element, the node is displaced and passes the forces to its neighboring nodes. The behavior of this configuration can be imagined similar to a spring-mass system. The described effect causes a deformation of the mesh. Boundary and initial conditions can be applied easily, so that the nodes of the boundary elements of an object stay unchanged. Also, very clear material boundaries exist in the Lagrange method. For the space outside the object, there is no extra mesh needed and mass conservation is automatically satisfied.

An example of this process is shown in Figure 3. A target and a bullet like object are modeled with a blue and a green material. The bullet (blue) has an initial velocity in the direction of the target. The left side shows the situation before the impact of the bullet. During the impact process the target (green) gets deformed and the deformation of the target is calculated as a result of the deformation of the Lagrange mesh of both objects at each time step.

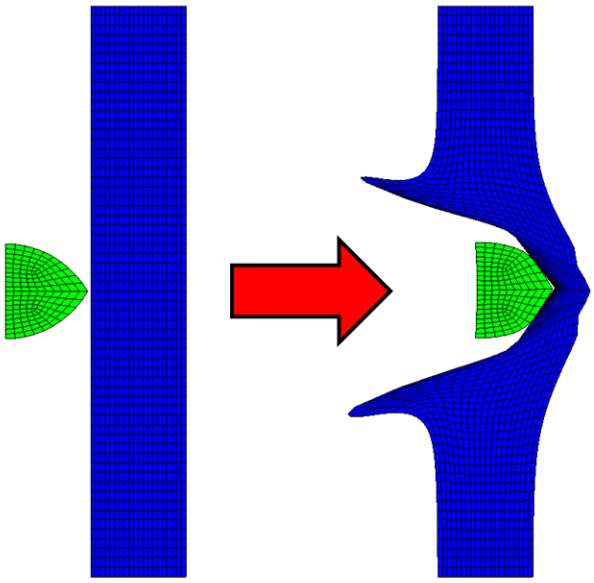

Figure 3. Lagrange method example: A bullet (green) and a target (blue), both with a Lagrange mesh. The left side shows the situation before and the right side after the impact of the bullet on the target. Adapted from [23].

In general, the Lagrange method is best suited for complex geometries like structures, projectiles and other solid bodies. A disadvantage of the Lagrange method is that strong mesh deformations may occur at high loads. Such a distorted mesh element can negatively influence the time-dependent solution because the time step is proportional to the size of the smallest element within the Lagrange mesh.

2) Euler: The Euler method differs in this way that the coordinates of the nodes are fixed and they fill the entire space. The material flows time-dependent through the mesh and changes the properties of the elements, while the spatial coordinates and nodes stay unchanged. That is the reason why no mesh distortion can occur at the Euler method. In contrast to the Lagrange method, the boundary nodes do not necessarily coincide with the material boundary conditions. This can result in difficulties in the application of boundary and interface conditions.

Figure 4 shows a bullet and a target modeled in the Euler frame. In contrast to the Lagrange frame, the whole simulation space consists out of a mesh. Part of this is the white space on both sides of Figure 4. Other parts of the simulation space are filled with material matching the objects they are meant to represent. After the impact, the material is spread over the mesh. The result shows a situation which fits Figure 3.

In general, the Euler method is used to represent fluids and

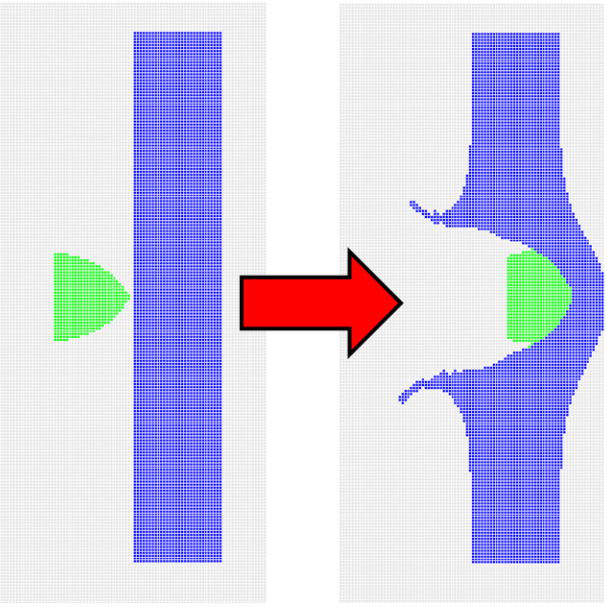

Figure 4. Euler method example: A bullet (green), a target (blue) and a (white) simulation space are modeled with an Euler mesh. The left side shows the situation before and the right side after the impact of the bullet on the target. Adapted from [23].

gases, especially for modeling the propagation of a blast wave as result of an explosion. If a pure simulation of solids is needed, the Euler method has the disadvantageous effect, that the stress tensor and the history of the material has to be transported through the mesh. In this case, Euler needs more computation performance and smaller elements to model the appearing blast wave correctly.

B. Material Models

1) Explosive: PETN and TNT serve as explosive ordnance through which the blast wave is generated at the beginning of the simulations. As equation of state, the Jones-Wilkins-Lee (JWL) equation is used. It describes the blast wave pressure as a function of the relative volume $\eta = \rho_0/\rho$ and the internal energy E [24]:

$$P = A\left(1 - \frac{\omega \cdot \eta}{R_1}\right) \cdot \mathrm{e}^{\frac{R_1}{\eta}} + B\left(1 - \frac{\omega \cdot \eta}{R_2}\right) \cdot \mathrm{e}^{\frac{R_2}{\eta}} + \omega \cdot \rho \cdot E \quad (2)$$

In this equation, A, B, R_1, R_2 and ω are material constants, which were determined in dynamic experiments.

Four different material models are defined for PETN in AUTODYN. These four models differ only in their densities $\rho_{0.88} = 0.88\ \mathrm{g/cm^3}$, $\rho_{1.26} = 1.26\ \mathrm{g/cm^3}$, $\rho_{1.50} = 1.50\ \mathrm{g/cm^3}$ and $\rho_{1.77} = 1.77\ \mathrm{g/cm^3}$. Simulations of explosives with these densities lead to nearly identical pressure profiles [25]. That is why the PETN material model of $\rho_{1.77}$ has been used in the first part of this work.

In the second part, TNT is used for simulation. Its behavior can be modeled with the same equation of state as for PETN. The JWL-equation will then have TNT specific material constants and the density of TNT $\rho_{\mathrm{TNT}} = 1.63\ \mathrm{g/cm^3}$ is used for correct calculations [24].

2) Ideal Gas: Air is a gas mixture mainly consisting of diatomic nitrogen and oxygen. In addition, a multitude of mono- or poly-atomic trace gases are contained in air. Furthermore, the ideal gas equation is a suitable equation of state for modeling air in numerical simulations:

$$P = \rho \cdot R_{\mathrm{s}} \cdot T \quad (3)$$

In this equation, P is the pressure, ρ the density of the gas, R_{s} a specific gas constant and T the temperature. An alternative but equivalent formulation of the previous equation is used in ANSYS AUTODYN for its internal calculations [24]:

$$P = (\gamma - 1) \cdot \frac{\rho}{\rho_0} \cdot E \quad (4)$$

In this alternative equation, γ is the ratio of the specific heat capacities at constant pressure $c_{\mathrm{P}}(T)$ and volume $c_{\mathrm{V}}(T)$. This ratio has the value $\gamma = 1.4$ under the conditions of ambient temperature at $T_{\mathrm{ref}} = 288\ \mathrm{K}$ and atmospheric pressure of $P_{\mathrm{atm}} = 101.3\ \mathrm{kPa}$. Based on these values, the reference density is $\rho_0 = 1.225\ \mathrm{kg/m^3}$ and the internal energy has the value $E = 253.4\ \mathrm{kJ/m^3}$.

A complete set of parameter-based data for a large interval of temperature values can be found in measurement-based tables [26] [27]. The corresponding values for γ can be extracted from this data. With these values, the internal energy E of a gas at a certain temperature T can be calculated by following equation:

$$E = \int_{T_{\mathrm{ref}}}^{T} c_{\mathrm{V}}(T) \cdot \mathrm{d}T \quad (5)$$

Table I is made up of the empirical and calculated data for a temperature range of 288 K to 3000 K. The density was calculated as a function of the temperature according to (3) at constant atmospheric pressure P_{atm}.

Since air is a gaseous material, it does not suffer shear stresses or negative pressures. That is the reason why no strength or failure model is necessary for the numerical simulation of air.

It should be noted that a heating process of air based on (3) is realized under the conditions, that either volume or pressure stay constant. A quick heating with constant volume will result in a very strong change of pressure. On the other hand, an expansion of the volume, which equals a decrease in density, leads to rapid heating with constant, ambient pressure.

3) Structural Material: Structured parts will be simulated by using the Lagrange method and the material steel-1006. The further material properties of steel are irrelevant, because

TABLE I. VALUES FOR DENSITY, INTERNAL ENERGY, HEAT CAPACITY AT CONSTANT VALUME AND PRESSURE OF AIR AT VARIOUS TEMPERATURES.

Temperature [K]	*Density* [g/cm^3]	*Internal Energy* [J/kg]	C_V [kJ/kg K]	C_P [kJ/kg K]
288	0.001225	2.068E+05	0.7173	1.0042
300	0.001177	2.143E+05	0.7177	1.0050
400	0.000882	2.865E+05	0.7262	1.0130
500	0.000706	3.600E+05	0.7423	1.0290
700	0.000504	5.127E+05	0.7876	1.0750
1000	0.000353	7.597E+05	0.8538	1.1410
1200	0.000294	9.341E+05	0.8873	1.1740
1500	0.000235	1.206E+06	0.9239	1.2110
1700	0.000208	1.393E+06	0.9419	1.2290
2000	0.000176	1.679E+06	0.9630	1.2500
2200	0.000160	1.872E+06	0.9731	1.2600
2500	0.000141	2.165E+06	0.9866	1.2740
2700	0.000131	2.364E+06	0.9942	1.2810
3000	0.000118	2.663E+06	1.0040	1.2910

it is only used to fill the object as a rigid body. An interaction between blast wave and object does not take place.

III. PROBLEM SET-UP

The following subsections describe the created problem set-up for the numerical simulation. Each element of the simulation space and all parts of the blast process are explained. The goal of this section is to get an understanding of how reality can be modeled in numerical simulations and what simplifications have been done to achieve that.

A. Basic Set-Up

1) Undisturbed Propagation: In order to measure the effects of an attenuation space for blast waves, a simulation set-up was developed, which ensures uniform and comparable conditions between individual simulations. This set-up is designed in such a way that the undisturbed propagation of the blast wave and its positive peak overpressure P_pop can be measured at various points in the simulated space. Subsequently, the individual parameters of the simulation are to be varied in order to be able to compare the effects on the pressure profile with the undisturbed case. Parameters to be changed are the thickness of the attenuation space, its temperature, density, pressure, position and shape. Other components of the simulation, such as the type of explosive and the type of space to be viewed, remain unchanged.

The approximate spatial configuration of the simulation is based on a certification standard for non-destructive requirements on special-safety vehicles. In order to validate the attenuation space, it is important to check the change of pressure on the vehicle by gauges. In this first view, the direct impact of the blast wave on the vehicle is negligible. That is the reason why the vehicle can be simulated as a rigid body like a dummy. This dummy vehicle has the shape of a sport utility vehicle (SUV), which is a good example for a security vehicle and is similar to military off-road vehicles.

The space, in which the blast wave should propagate, will be modeled with the Euler method. The Euler Multi-Material solver is used to fill a space with air under ambient temperature and atmospheric pressure. The created space is designed in such a way that it can represent all important elements of the propagation of the blast wave in the direction of the vehicle. It has a length of $l = 13.00$ m, a width of $b = 6.00$ m and a height of $h = 3.00$ m. The individual hexahedral elements of the mesh in the Euler space have an edge length of 0.05 m. Accordingly, the space is filled with 1.872 million elements. The entire set-up of the simulation is shown in Figure 5.

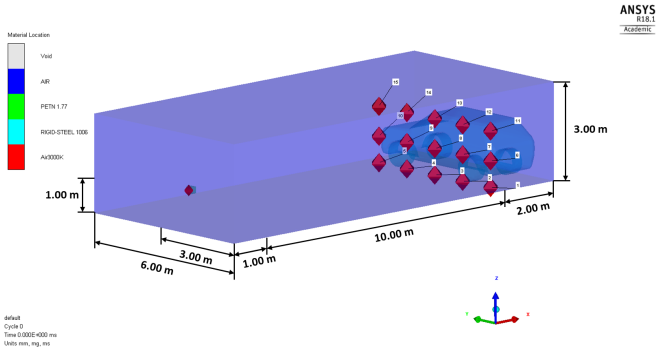

Figure 5. The simulation space filled with different materials and a vehicle model from an oblique, lateral perspective with gauges and PETN explosive.

The entire simulation space is mainly filled with air (blue space) at ambient condition and with a vehicle model (dark blue). The view on this simulation space is from an oblique, lateral perspective. The sides of the simulated space are provided with boundary conditions, which allow the blast wave to flow out. In this way, a disturbing reflection of the blast wave on these sides is avoided. Only the floor of the space is excluded from this condition, so that the blast wave is reflected. By applying this boundary condition, the computation effort is reduced and the same result is achieved as if the room was an infinite space.

At the end of the long side of this space, the vehicle is positioned in such a direction that it will be hit on the side by the blast wave. In Figure 5, the PETN explosive with its detonation point is located to the left of the front of the space. The explosive is placed in a distance of 10 m away from the vehicle, exactly centered and hovering in 1 m height. The hovering state is realized in the simulation just by placing the explosive at this coordinate. Because of typically very short durations in high-speed dynamics every influence of gravitational forces on the position of the explosive can be neglected. In reality, the localization of the explosive would be realized by a platform of easily destructible material, which holds the explosive. The volume of the explosive is chosen in such a way that it equals an amount of 15 kg TNT. The TNT

equivalent of PETN is approximately 1.2, that is why 12.5 kg of PETN are required [28]. In accordance with the certification standard, the explosive is chosen in the shape of a cube. The edge length a of this cube for a given mass $m_{\mathrm{PETN}} = 12.5$ kg and density $\rho_{1.77}$ can be calculated by its volume V:

$$a = \sqrt[3]{V} = \sqrt[3]{\frac{m_{\mathrm{PETN}}}{\rho_{1.77}}} \approx 0.19 \text{ m} \tag{6}$$

The detonation point for the explosive is centered on the surface which is located on the side facing away from the vehicle. This results in a blast wave moving in the direction of the vehicle. Left side to the front of Figure 5 shows the PETN cube with its red detonation point.

The measurement of the pressure profile of the blast wave is done by fifteen pressure gauges. In Figure 5, the red dots on the right side represent these gauges at which the pressure can be measured. They are located above each other, three rows of five gauges directly in front of the rigid vehicle. Each gauge can collect data of various physical properties during the entire time of simulation.

The presented set-up can be used to perform simulations of the undisturbed propagation of blast waves.

2) Disturbed Propagation: In a next step, an attenuation space is placed directly in front of the vehicle. This space consists of front and back faces with constant area and a variable thickness in the direction of the blast. Furthermore, position, shape, temperature, density and pressure are changeable. This set-up with the newly introduced attenuation space is shown in Figure 6.

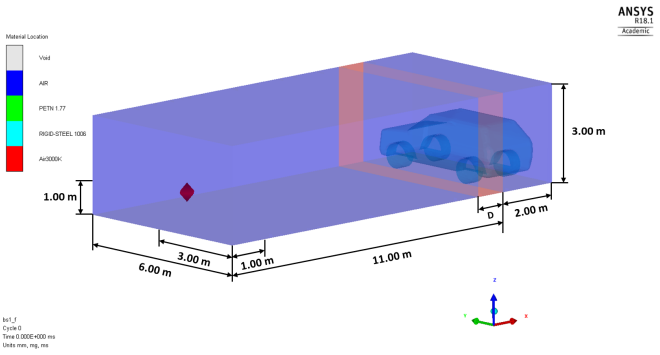

Figure 6. The simulation space filled with different materials and a vehicle model from an oblique, lateral perspective with a detonation point on the left side. The reddish space on the right side represents the attenuation space.

The entire simulation space is filled with different materials and a vehicle model from an oblique, lateral perspective. The mainly blue space in this figure is filled with air at ambient condition. The reddish space on the right side represents the attenuation space. This space has a thickness D, which can be set arbitrarily in the direction of the blast. Furthermore, shape and density are variable. The previously described gauges exist in this set-up as well and they record changes in pressure during the simulation. For the sake of clarity, the gauges are hidden in this figure.

B. Advanced Set-Up

The simulation scenario described before is a very basic and artificial attempt to estimate the effect of a blast attenuation mechanism. However, due to the high strength of the 12.5 kg PETN explosive used in the previous set-up, the set-up shows an upper limit of its attenuation capability.

To validate a more realistic scenario the basic set-up is modified. A huge PETN explosive ordnance is a good choice for the certification of the demolition of a vehicle but in reality other threats like high-angle weapons with explosive ammunition are more plausible. For example, an incoming mortar grenade next to a security vehicle. Such a mortar grenade is a weapon not only used by military units but also by insurgents and terrorist. It is a very simple weapon with cheap ammunition, which are distributed vastly due to the cold war. It also satisfies the requirements for a flexible weapon as described in the introduction. The actual form of this weapon was developed to support infantry units as a light and mobile weapon [29]. It fills the gap between artillery and grenades, so that the troops can adjust flexibly and quickly to possible threats.

The advanced scenario will use a representation of a mortar grenade as explosive instead of the huge 12.5 kg PETN explosive ordnance. The remaining configuration stays the same.

1) Mortar Ammunition: Mortars are available as lighter or heavier versions. The lighter version normally has a caliber of 81 mm with a range of about 5000–6000 m. A heavy mortar has a increased weight but it can fire its 120 mm shells to a distance of about 7000–8000 m. High firing distances and light overall weight of about 50–120 kg make the mortar a flexible and easy transportable weapon [29].

As shown in Figure 7, the body of a mortar grenade consists of a fin stabilized tail and a shell. Essentially, the shell of the mortar grenade carries the explosive with the fuze at the top of the shell. Depending of what kind of fuze is used it is possible to let the grenade explode by impact or above the ground [30]. The grenade shown in Figure 7 is a light version of a Russian 120 mm grenade, which should be used as an example for the following simulation. The heavy grenade has an explosive filler with weight of $m_{\mathrm{grenade}} = 2.6$ kg TNT and a overall length of $l_{\mathrm{overall}} = 0.665$ m [31].

2) Modeling a Mortar Grenade: To model such a grenade in ANSYS AUTODYN, the volume of the explosive filler is needed. Its value can be calculated by using the simple relationship between density ρ_{TNT}, volume V and mass m:

$$V = \frac{m_{\mathrm{grenade}}}{\rho_{\mathrm{TNT}}} \approx 1.58 \cdot 10^{-5} \text{ m}^3 \tag{7}$$

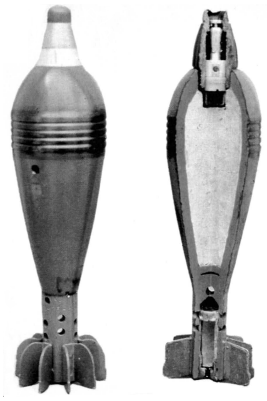

Figure 7. Illustration of a light 82 mm high explosive mortar grenade as used during cold war and today. The right side shows a cross-section with the high explosive material filler in the middle and the fuze on top of it [31].

For the sake of simplicity, in the simulation of the mortar grenade this volume can be represented by a cuboid with square base. The edge length of the square base is $a = 0.10$ m and $h = 0.15$ m for its height or longest dimension. These dimensions lead to a volume which satisfies the calculation from equation (7).

For the simulation, an outer shell of the mortar grenade is not needed because the release of shrapnel is not relevant. Only the blast wave is needed to get an impression about the interaction with the attenuation space. The fuze of the grenade can be modeled as a detonation point on top of the cuboid. The described design is realized in Figure 8.

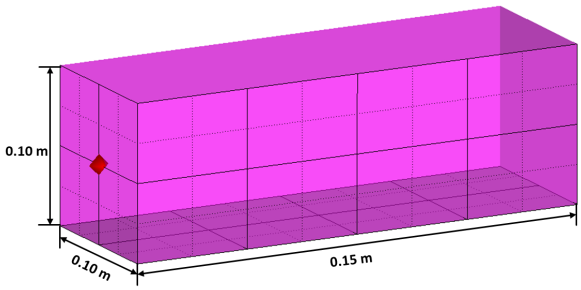

Figure 8. Simplified computer model of a mortar grenade. The space in the magenta color is filled with TNT and the red point on top is the detonation point.

The modeled grenade in Figure 8 is filled with TNT, which is represented by the color magenta. It also has a detonation point on top, shown as red dot. This simple representation of the grenade shown in Figure 7 meets all requirements to allow a simulation.

3) Simulation Space: The modeled mortar grenade will be placed in the simulation space instead of the huge PETN explosive ordnance. It will be placed in such a way that the normal component of the surface, where the detonation point is located, points toward the ground of the simulation space. This imitates the behavior of a real mortar grenade because its velocity direction would point toward the ground before impacting and exploding.

In Figure 9, the mortar grenade model from Figure 8 is part of the advanced simulation set-up. Again, the grenade is represented by a magenta color with the detonation point pointing to the ground.

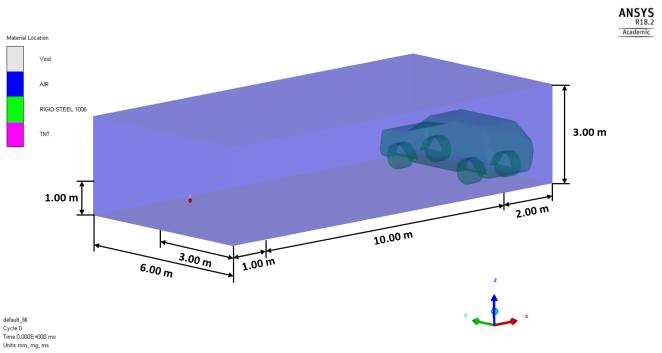

Figure 9. The simulation space filled with air and a vehicle model from an oblique, lateral perspective. On the left side of the space a simplified mortar grenade model with a detonation point (red dot) was inserted.

The configuration of this set-up is the same as in the basic case. Only the explosive ordnance is replaced. With this set-up the undisturbed propagation of the blast wave and a propagation through an attenuation space can be investigated. This offers the possibility to check if the attenuation of the blast wave will be achieved in the case of a smaller and more realistic explosive threat for the vehicle.

IV. Results and Discussion

The simulation results between the undisturbed and the attenuated blast wave propagation with the basic and advanced set-up are described below. The results are compared and discussed.

A. Undisturbed Propagation of the Basic Set-Up

The numerical calculations of the undisturbed blast wave propagation agree well with the expected ideal behavior. After the start of the simulation, the detonation of the PETN explosive leads to a successive conversion of the explosive. This results in a blast wave, which propagates radially away from its source. A part of the expanding blast wave is reflected on the ground and overlaps with the wave front. Hence, spaces of the blast wave with higher pressure are created, which can be observed near the ground.

Figure 10 shows this situation in the simulated test set-up. The blast wave is represented by vector arrows of the velocity

component in a color coding. The color changes from red to blue, as does the speed from high to low. The shown blast wave expands radially away from the explosive ordnance towards the vehicle. A part of the wave front is superimposed by the reflection on the ground.

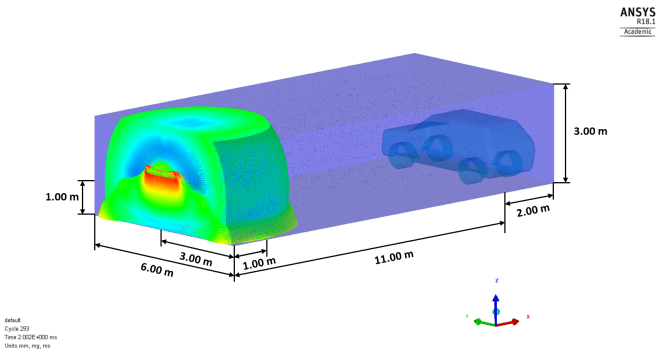

Figure 10. The simulation space filled with different materials and a vehicle model from an oblique, lateral perspective. A blast wave expands radially outwards from the left front side towards the vehicle.

If the blast wave reaches the vehicle, the pressure gauges will record the pressure change. For the evaluation, the data of gauges 3 (g3), 8 (g8) and 13 (g13) are used. These gauges are located exactly in the middle of the dimension along the y-axis of the simulation set-up. Along z-direction they are located at the ground, in middle height and on top of the vehicle. The pressure profile of the recorded data is shown in Figure 11. The overall profile of the measured pressure is in good accordance to the profile of the ideal shock wave from Figure 1. The peak overpressure values can be extracted from the recorded data. It is important to notice that these peak overpressure values are valid with respect to the atmospheric pressure of 100 kPa.

The gauges measured a peak overpressure of $P_{\mathrm{g3}} = 62.87\ \mathrm{kPa}$ at the bottom, $P_{\mathrm{g8}} = 62.45\ \mathrm{kPa}$ in the middle and $P_{\mathrm{g13}} = 62.94\ \mathrm{kPa}$ on top. Vehicles that are hit by a blast wave with a pressure amplitude of about 62 kPA are overturned and heavily damaged. Buildings cannot resist this overpressure as well: wood framed buildings collapse, steel framed buildings receive serious damage and reinforced concrete structures suffer severe damage [32] [33].

B. Heating under Atmospheric Pressure of the Basic Set-Up

For the next step, a part of the simulation space was filled with a cuboid-shaped volume of modified air at which the feasibility of the blast wave attenuation can be verified. The volume of this space is defined as the entire height and width of the simulation space. The thickness of the space was set to $D = 1.00\ \mathrm{m}$ and placed in a distance of d away from the vehicle, which in this case equals the amount of the thickness. Through that, the modified volume fills the free space without touching any part the vehicle. To emulate a rapid heating

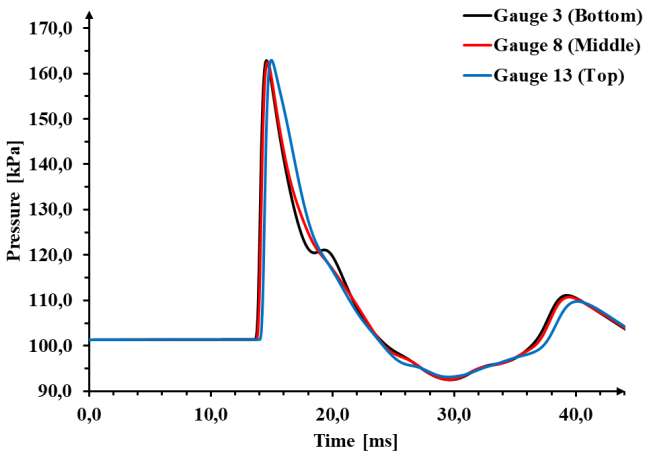

Figure 11. Simulated time-dependent pressure profile of the blast wave of the simulation set-up. After its release through the explosion, the wave propagates spatially and reaches the vehicle after $t_{\mathrm{a}} \approx 14\ \mathrm{ms}$. As in the ideal profile, a positive and negative phase of the pressure is visible.

under atmospheric pressure, the ambient air was replaced by air which matches the properties and internal energy of air at a temperature of $T = 3000\ \mathrm{K}$ according to Table I.

Three recorded pressure profiles of the blast wave, which has to cross such a volume in the simulation space, are shown in Figure 12.

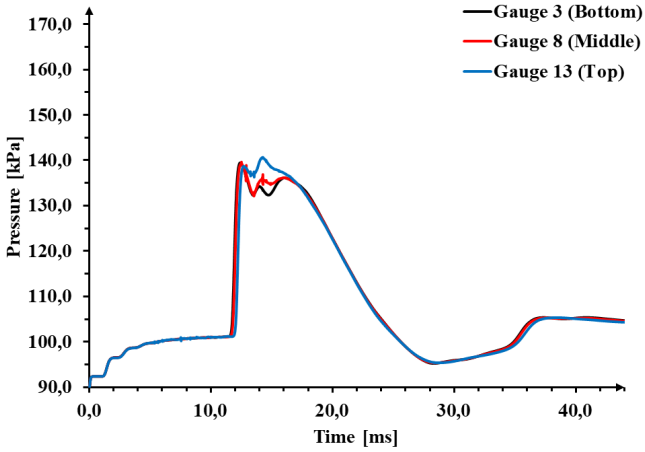

Figure 12. Simulated time-dependent pressure profile of the blast wave after crossing the attenuation space. The pressure profile shows an attenuation in the direction of the maximum pressure.

At the start of the pressure recording, the used method of heating will result in a slight vacuum because parts of the adjacent ambient air flow into the heated region because of the reduced density. The pressure stabilizes until the time of arrival of $t_{\mathrm{a}} \approx 14\ \mathrm{ms}$. When the blast wave reaches the gauges, a sudden increase in pressure occurs like in the undisturbed

case. In contrast, the measured peak overpressure at the gauges is lower and has the following values $P_{\mathrm{g3,heat}} = 40.87$ kPa, $P_{\mathrm{g8,heat}} = 41.98$ kPa and $P_{\mathrm{g13,heat}} = 45.79$ kPa.

In direct comparison, the relative differences of these peak overpressure values are $\Delta P_{\mathrm{g3,rel}} = 35.0\ \%$, $\Delta P_{\mathrm{g8,rel}} = 32.8\ \%$ and $\Delta P_{\mathrm{g13,rel}} = 27.2\ \%$ lower than the undisturbed case. These lower peak overpressure values are the consequence of the propagation of the blast wave through the attenuation space. Because of that, the object to be protected experience lesser damage and an attenuation of the blast wave through a second, transient medium is provable in the simulation. Furthermore, it can be seen in the pressure profile of Figure 12 that the pressure stays at a lowered level where the sharp peak used to be. Finally, the pressure drops off similar to the undisturbed case.

The three different gauges show small differences in their individual profiles. In contrast to the undisturbed case, the peak pressure rises from bottom to top gauge. This can be an indication for a disturbance of the radial, symmetric propagation of the blast wave. An explanation can be the diffraction of a part of the blast wave in the direction of the top gauge. Another reason can be that a fraction of the propagating blast wave is reflected from the ground in an upper direction towards the top gauge.

Because the attenuation space provided first results, the influence of its parameters temperature, thickness and distance was verified by a parameter study. The first changed parameter was the position d of the attenuation space relative to the vehicle. The change was applied in steps of $\Delta d = 1$ m. To compare the difference, the peak overpressure values of the undisturbed case were related with the attenuated values as normalized overpressure values. Figure 13 shows these normalized overpressure profiles.

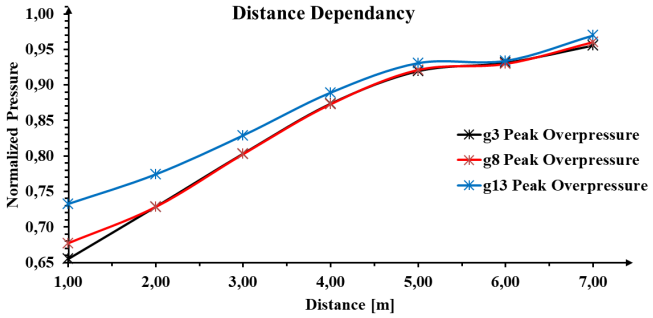

Figure 13. Distance-dependent normalized overpressure profile of the simulated attenuation space. The simulation data of the bottom, middle and top gauges are plotted and connected with smoothed curves.

The normalized overpressure rises with increasing distance from the vehicle. The individual records of the three gauges are similar to each other. But at near distances $d < 4.00$ m, the profile of the top gauge (g13) shows a recognizable difference to the other two gauges. This difference decreases with increasing distance d. This behavior can also be an indication for diffraction of the blast wave or the reflection of parts of the wave from the ground towards the top. In conclusion, to get a high attenuation of the blast wave, the attenuation space should be placed as near as possible to the asset to be protected.

The next parameter variation was done under the same conditions as before. With the attenuation space near the vehicle, the thickness D of the space was altered. The resulting normalized overpressure profile is plotted in Figure 14. It shows that the normalized overpressure decreases with increasing thickness and stabilizes at values of $D > 1.50$ m. For best results, the thickness should be at least $D = 1.50$ m.

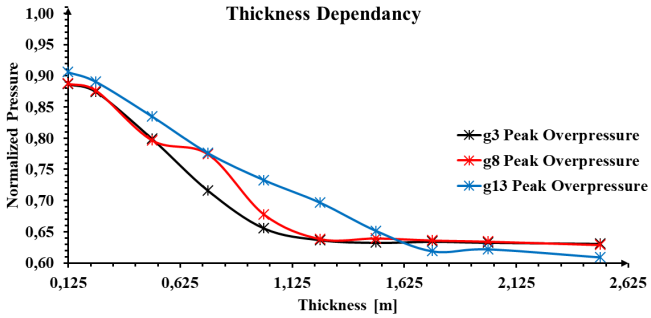

Figure 14. Thickness-dependent normalized overpressure profile of the simulated attenuation space. The simulation data of the bottom, middle and top gauges are plotted and connected with smoothed curves.

In a next step, the temperature was changed as a parameter. To do that, the same conditions as before apply with a change in temperature. Figure 15 shows these profiles.

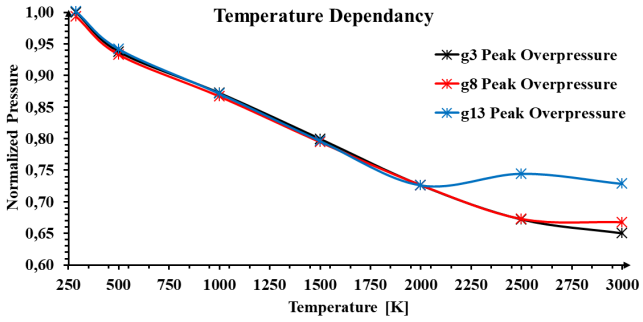

Figure 15. Temperature-dependent normalized overpressure profile of the simulated attenuation space. The simulation data of the bottom, middle and top gauges are plotted and connected with smoothed curves.

In the case of changed temperature, the normalized overpressure decreases with increasing temperature. The measurements of the three gauges behave alike to temperatures of $T > 2000$ K. From that temperature on, the values of middle and top gauge differ from the bottom gauge. Again, this can be indicating a diffraction of the blast wave from bottom to top.

Overall, the attenuation is the better the higher the temperature is.

The evaluation of this parameter study shows the following values as the optimal setting for the attenuation space in the simulation set-up: Thickness $D = 1.50$ m, distance $d = 1.50$ m, temperature $T = 3000$ K and the properties of air at this temperature according to Table I. With this setting of parameters and the results, the best overpressure values in the simulation could be extracted: $P_{\mathrm{g3,best}} = 39.43$ kPa, $P_{\mathrm{g8,best}} = 39.61$ kPa and $P_{\mathrm{g13,best}} = 40.67$ kPa. The relative differences to the undisturbed case correspond to: $\Delta P_{\mathrm{g3,best}} = 37.3$ %, $\Delta P_{\mathrm{g8,best}} = 36.5$ % and $\Delta P_{\mathrm{g13,best}} = 35.4$ %.

In contrast to the undisturbed case, a lesser pressure difference of about 40 kPa results in less drastic consequences for the vehicle being hit. In this magnitude, there is no overturning of vehicles and a complete destruction of the vehicle is no longer to be expected. It is shown that under the correct application of the attenuation space in the simulation a noticeable attenuation of the blast wave can be detected.

Finally, it should be noted that the simulation differs from the real conditions in which a volume can be heated. At first, the heated and simulated space is discretely separated from the environment. Any change of the properties in the attenuation space does not change anything in the surrounding ambient air before the simulation starts. Second, the heating takes place in the case of constant atmospheric pressure in a very short time. In reality, interactions with the surrounding air, in particular diffusion, are to be expected during such a heating process. Additionally, the increase in temperature of $T > 3000$ K leads to an ionization of air. Such an ionization is accompanied by a change in density, which cannot be shown in the simulation. It is also important that steel can melt at such high temperatures. Therefore, the attenuation space must not be in direct contact with the object to be protected. In reality, it is necessary to examine how such rapid heating of ambient air affects the asset, as well as people and objects nearby.

C. Results of the Advanced Set-Up

The simulation of the modified set-up starts with the ignition of the modeled mortar grenade. This leads to a similar blast wave behavior as in Figure 10. The shown blast wave expands radially outwards from the left front side towards the vehicle. Again, a part of the wave front is superimposed by the reflection on the ground. When the blast wave arrives at the vehicle, changes of pressure will be recorded by pressure gauges. As before, only the gauges located in the middle of the ground, in middle height and on top of the vehicle are used for collecting and evaluating data.

The pressure profile of the collected data in the undisturbed case caused by the mortar grenade is shown in Figure 16.

Compared to the ideal shock wave behavior from Figure 1 and the undisturbed propagation from Figure 13 there are some differences. The rise of the amplitude is not as steep as in the both other cases. The reason for this is that the blast wave has already slowed down and is increasingly turning into a compression wave. The cause of the slowdown is the smaller amount of explosive at the same distance as before. Also, the amplitude of the blast wave is not as high as with the huge PETN explosive.

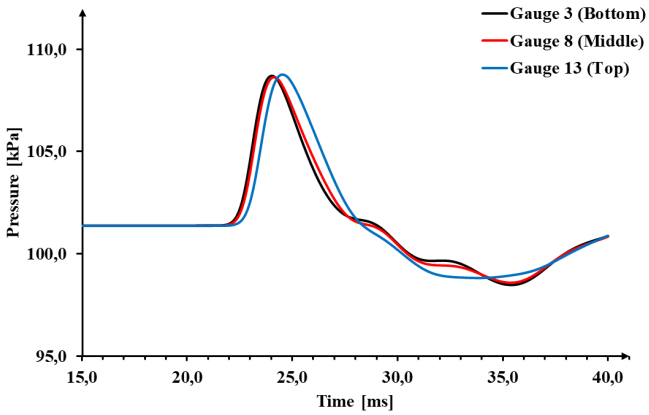

Figure 16. Simulated time-dependent pressure profile of the blast wave of the simulation set-up. After the explosion of the mortar grenade, the wave propagates spatially and reaches the vehicle after $t_{\mathrm{a}} \approx 22$ ms. As in the ideal profile, a positive and negative phase of the pressure is visible.

The results are peak overpressure values of $P_{\mathrm{g3,mor}} = 8.70$ kPa, $P_{\mathrm{g8,mor}} = 8.63$ kPa and $P_{\mathrm{g13,mor}} = 8.76$ kPa. At these overpressure values the following damages are expected: Glass failure, houses are made inhabitable, slight distortion of the steel frames of clad buildings and slight to serious injuries of persons [32] [33]. The amplitude is not strong enough to overturn a vehicle. It is to be expected that a security vehicle will withstand such a blast wave.

To get a comparable result about a possible attenuation of the blast wave, the set-up was provided with an attenuation space. Like before a cuboid-shaped volume of modified air with the same properties ($T = 3000$ K) was used. The recording of the resulting pressure profile is shown in Figure 17.

From slight underpressure at the beginning, the pressure stabilizes in Figure 17 until the time of arrival of $t_{\mathrm{a}} \approx 22$ ms. When the blast wave reaches the gauges, a steep but not to sudden increase in pressure occurs. This indicates that the wave has been weakened. There are also some minor peaks in the profile of gauge 8 and 13. An explanation could be an turbulence in the propagation of the blast wave. However, because of the regular, common intervals at the profiles of both gauges it might be an error in the calculations of the simulation software. Compared to each other only the profile of gauge 13 has slightly higher values.

In contrast to the undisturbed case shown in Figure 16 the measured peak overpressure at the gauges is lower and has the following values $P_{\mathrm{g3,mor,h}} = 5.75$ kPa, $P_{\mathrm{g8,mor,h}} = 5.77$ kPa and $P_{\mathrm{g13,mor,h}} = 6.12$ kPa. In direct comparison with the

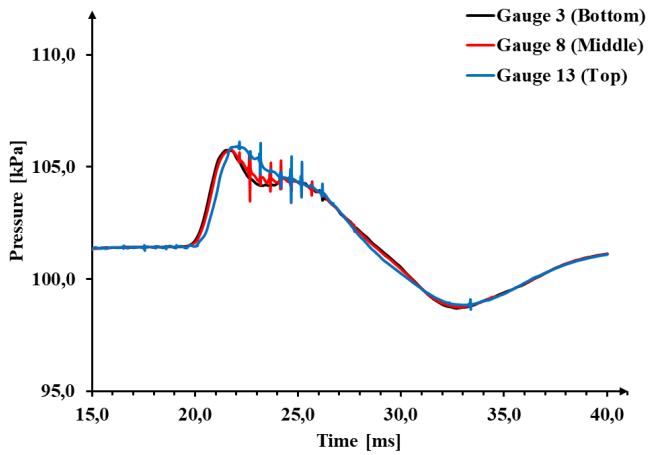

Figure 17. Simulated time-dependent pressure profile of the blast wave after crossing the attenuation space. The pressure profile shows an attenuation in the direction of the maximum pressure.

values $P_{\mathrm{g3,mor}}$, $P_{\mathrm{g8,mor}}$ and $P_{\mathrm{g13,mor}}$ the relative differences of these peak overpressure values are $\Delta P_{\mathrm{g3,mor,rel}} = 33.9\ \%$, $\Delta P_{\mathrm{g8,mor,rel}} = 33.2\ \%$ and $\Delta P_{\mathrm{g13,mor,rel}} = 30.1\ \%$ lower. Like in the set-up before an effect of the attenuation space is measurable.

V. Conclusion

Assets of armed and security forces are threatened by terrorists and insurgents, especially by explosive weapons. The armor of these assets effectively protects them against splinters and shrapnel, but not against the blast wave of the explosion. Therefore, in order to reduce the danger of explosions, the blast wave has to be weakened before reaching the asset. This can be achieved by rapidly heating a region of normal ambient air to produce a second, transient medium at which the blast wave is attenuated.

In this work, a simulation set-up was developed for this purpose, which could be used to check whether the heating of a volume of air at a constant ambient pressure leads to a reduction in the peak pressure of a blast wave. Through this set-up the undisturbed propagation of the blast wave could be compared with the disturbed case. An attenuation of the blast wave was measurable. A further examination through a parameter study led to the following findings.

The measurable attenuation of the blast wave is the more effective the higher the temperature, the nearer the attenuation space to the asset and the more the thickness becomes a value of $D > 1.50\ \mathrm{m}$. In addition, it was possible to find indications of diffraction or reflection of the blast wave.

With the found set of best parameters a simulation of the basic set-up was performed. It led to a reduction of the peak overpressure of the blast wave with an achieved attenuation of about 35.0 %. With respect to the very high overpressure values of about $63\ \mathrm{kPa}$, this is a reduction which can decrease the damage of a vehicle significantly.

Based on the preceding findings, the basic set-up was improved to a more realistic scenario. Instead of using a huge PETN explosive ordnance, a simplified model of a mortar grenade was developed. This model reflects the properties of a vastly distributed ammunition type, which is a real threat for security forces in many foreign operations. This model allowed to do an advanced simulation of an undisturbed propagation of the blast wave and a propagation through an attenuation space. As result, an attenuation of the blast wave in this more realistic scenario of up to 33.9 % was achieved.

As this research has shown, it is theoretically possible to attenuate the blast wave by second, transient medium. In order to further investigate its effectiveness, the next step should be to examine how the shape and a more accurate selection of the gas parameters affect the attenuation. In particular, it must be checked whether a high attenuation can be achieved by new material models such as, for example, air with ionization or an air-dust mixture. An experimental verification of such an attenuation space of heated air would be particularly revealing for a technical realization. Therefore, it is interesting to ask whether the presented concept can be developed with a proper configuration of the second, transient medium to a kind of attenuation shield against blast waves.

References

[1] B. Hillig, A. Ramezani, and H. Rothe, “Verification of the Theoretical Feasibility of Shock Wave Attenuation by Means of a Second Transient Medium for Protecting Vehicles Against Blasts,” in SIMUL 2017 : The Ninth International Conference on Advances in System Simulation (SIMUL 2017) Athens, Greece. IARIA, Oct. 2017, pp. 68–73, ISBN: 978-1-61208-594-4.

[2] B. J. Tillotson and M. A. Loudiana, “Method and apparatus for shockwave attenuation,” U.S. Patent No. 8,806,945, 2014.

[3] R. Cobbold, “The Effects of Operations Other Than War-Fighting on the Participants,” in Royal United Services Institute for Defence and Security Studies, Conference, Paris, France, Jun. 2005, (Keynote Address).

[4] P. F. Herrly, The Impact of Peacekeeping and Stability Operations on the Armed Forces. Heritage Foundation, 2005.

[5] J. Kress and S. Grogger, “The domestic ied threat,” Institute for National Strategic Studies, National Defense University, Washington, Tech. Rep., 2008.

[6] D. E. Carlucci and S. S. Jacobson, Ballistics: theory and design of guns and ammunition. CRC Press, 2013.

[7] J. A. Zukas, W. Walters, and W. P. Walters, Explosive effects and applications. Springer, New York, 1998.

[8] I. Sochet, Blast Effects: Physical Properties of Shock Waves. Springer, 2017.

[9] W. E. Baker, Explosions in air. University of Texas press, 1973.

[10] O. Igra, J. Falcovitz, L. Houas, and G. Jourdan, “Review of methods to attenuate shock/blast waves,” Progress in Aerospace Sciences, vol. 58, 2013, pp. 1–35.

[11] G. L. Gettle and V. H. Homer, “Acoustic/shock wave attenuating assembly,” U.S. Patent No. 5,394,786, 1995.

[12] K. Kitagawa, M. Yokoyama, and M. Yasuhara, "Attenuation of shock wave by porous materials," in Shock Waves, Z. Jiang, Ed. Berlin, Heidelberg: Springer Berlin Heidelberg, 2005, pp. 1247–1252.

[13] J. L. Waddell and J. F. Gordon, "Acoustic shock wave attenuating assembly," U.S. Patent No. 8,316,752, 2012.

[14] E. Lozano and P. Vilem, "Design and testing of blast shields for different blasting applications," Blasting and Fragmentation, vol. 9, no. 1, 2015, pp. 1–18.

[15] M. Sommerfeld, "The unsteadiness of shock waves propagating through gas-particle mixtures," Experiments in Fluids, vol. 3, no. 4, 1985, pp. 197–206.

[16] O. Igra, G. Ben-Dor, F. Aizik, and B. Gelfand, "Experimental and numerical investigation of shock wave attenuation in dust-gas suspensions," in Shock Waves@ Marseille III. Springer, 1995, pp. 49–54.

[17] J. Zukas, Introduction to hydrocodes. Elsevier, 2004, vol. 49.

[18] A. Hamouda and M. Hashmi, "Modelling the impact and penetration events of modern engineering materials: characteristics of computer codes and material models," Journal of materials processing technology, vol. 56, no. 1-4, 1996, pp. 847–862.

[19] D. J. Benson, "Computational methods in lagrangian and eulerian hydrocodes," Computer methods in Applied mechanics and Engineering, vol. 99, no. 2-3, 1992, pp. 235–394.

[20] M. Oevermann, S. Gerber, and F. Behrendt, "Euler–lagrange/dem simulation of wood gasification in a bubbling fluidized bed reactor," Particuology, vol. 7, no. 4, 2009, pp. 307–316.

[21] D. Hicks and L. Liebrock, "Sph hydrocodes can be stabilized with shape-shifting," Computers & Mathematics with Applications, vol. 38, no. 5, 1999, pp. 1–16.

[22] X. Quan, N. Birnbaum, M. Cowler, B. Gerber, R. Clegg, and C. Hayhurst, "Numerical simulation of structural deformation under shock and impact loads using a coupled multi-solver approach," in Proceedings of 5th Asia-Pacific Conference on Shock and Impact Loads on Structures, 2003, pp. 12–14.

[23] A. Ramezani, B. Hillig, and H. Rothe, "A Coupled CFD-FEM Analysis to Simulate Blast Effects on High Security Vehicles Using Modern Hydrocodes," in SIMUL 2017 : The Ninth International Conference on Advances in System Simulation (SIMUL 2017) Athens, Greece. IARIA, Oct. 2017, pp. 74–81, ISBN: 978-1-61208-594-4.

[24] A. AUTODYN, "Autodyn user's manual, release 18.0," 2017.

[25] M. Johansson, O. P. Larsen, L. Laine, and R. S. AB, "Explosion at an intersection in an urban environment–experiments and analyses," in Proceedings of the 78th Shock and Vibration Symposium, Philadelphia, PA, USA, 2007.

[26] E. W. Lemmon, R. T. Jacobsen, S. G. Penoncello, and D. G. Friend, "Thermodynamic properties of air and mixtures of nitrogen, argon, and oxygen from 60 to 2000 k at pressures to 2000 mpa," Journal of physical and chemical reference data, vol. 29, no. 3, 2000, pp. 331–385.

[27] J. H. Keenan, J. Chao, and J. Kaye, "Gas tables: international version," in Gas tables: international version. John Wiley & Sons, 1983.

[28] D. O. Dusenberry, Handbook for blast resistant design of buildings. John Wiley & Sons, 2010.

[29] I. V. Hogg, Mortars. The Crowood Press Ltd, 2001.

[30] I. V. Hogg, The Illustrated Encyclopedia of Ammuntion. Chartwell Books, 1985.

[31] I. V. Hogg, Ammunition: Small Arms, Grenades, and Projected Munitions. Greenhill Books/Lionel Leventhal, 1998.

[32] V. Clancey, "Diagnostic features of explosion damage," in 6th Int. Meeting of Forensic Sciences, Edinburgh, 1972.

[33] U. N. R. Commission et al., "Fire dynamics tools (fdts): Quantitative fire hazard analysis methods for the us nuclear regulatory commission fire protection inspection program," NUREG-1805, December, 2004.